Eur. Phys. J. D **44**, 9–16 (2007)
DOI: 10.1140/epjd/e2007-00147-0

THE EUROPEAN PHYSICAL JOURNAL D

Oscillator strength measurements of the 3p → nd Rydberg transitions of sodium

M.A. Baig[a], S. Mahmood[b], M.A. Kalyar, M. Rafiq, N. Amin, and S.U. Haq

Atomic and Molecular Physics Laboratory, Department of Physics, Quaid-i-Azam University, Islamabad 45320, Pakistan

Received 22 December 2006 / Received in final form 16 February 2007
Published online 4 May 2007 –

Abstract. We report new measurements of the oscillator strengths of the $3p\ ^2P_{3/2} \rightarrow nd\ ^2D_{5/2,3/2}$ and $3p\ ^2P_{1/2} \rightarrow nd\ ^2D_{3/2}$ Rydberg transitions of sodium using a thermionic diode ion detector in conjunction with the Nd:YAG pumped dye lasers. The $ns\ ^2S_{1/2}$ and $nd\ ^2D_{5/2,3/2}$ Rydberg series have been recorded via two-step excitation, from the $3p\ ^2P_{3/2}$ and $3p\ ^2P_{1/2}$ intermediate states. Employing the saturation technique, the photoionization cross sections from the $3p\ ^2P_{3/2}$ and $3p\ ^2P_{1/2}$ intermediate states at the first ionization threshold are determined as 7.9(1.3) Mb and 6.7(1.1) Mb respectively. The f-values of the Rydberg transitions are calibrated with the photoionization cross section measured at the first ionization threshold and compared with the earlier data.

PACS. 32.30.Jc Visible and ultraviolet spectra – 32.80.Rm Multiphoton ionization and excitation to highly excited states (e.g., Rydberg states)

1 Introduction

The sodium atom has an inert core and a single valence electron, which is similar to that of hydrogen atom, possessing $3s\ ^2S_{1/2}$ ground state configuration. The energy positions of the Rydberg states of sodium have been extensively studied since the advent of narrow bandwidth tunable dye lasers and the results have been discussed in a number of books [1–5], but comparatively little information is available about the oscillator strengths of the highly excited states. Measurements of the absolute optical oscillator strengths provide information about the electronic transition probabilities for the valance or inner shell excitations and ionization processes. The oscillator strength of a transition is proportional to the square of dipole matrix elements and is a dimensionless number that is useful for comparing different transitions. The determination of oscillator strength of Rydberg transitions require the absolute value of the photoionization cross section at the ionization threshold to be used for calibration.

A number of groups have calculated the optical oscillator strength of the resonance transitions of sodium ($3s \rightarrow 3p$) but very little data is available for the higher members of the series. Manson [6] predicted the existence of a minima in the continuum generalize oscillator strengths for different atoms and calculated the oscillator strengths for the $3s \rightarrow 3p$ transitions of sodium. Weisheit [7] calculated the oscillator strengths and the ground state photoionization cross section for the principal series of the alkali metals (Na, K, Rb and Cs). Shuttleworth et al. [8] determined the cross sections and the oscillator strengths of the $3s \rightarrow 3p$ transitions of Na and the angular dependence of these parameters for different incident electron energies was also measured. Vuskovic and Srivastava [9] used a crossed-electron-beam-metal-atom-beam scattering technique to measure the cross sections at different incident energies by varying the scattering angles for different states of sodium. Using the theoretical and experimental data, they extrapolated the differential cross sections between the angular regions of 0–10 degrees and 120–180 degrees and determined the oscillator strengths of the resonance transitions of sodium. Barrientos and Martin [10] applied the quantum defect orbital method to compute the oscillator strengths and photoionization cross sections of the alkali metals. Mitroy [11] calculated the oscillator strength from the cross sections for the $3s \rightarrow 3p$ transitions of Na in a four state approximation ($3s$, $3p$, $4s$, $3d$) at 22.1 eV, 54 eV and 150 eV energies. Bielschowsky et al. [12] both theoretically and experimentally investigated the generalized oscillator strength for $2p$–$3s$ and $3s \rightarrow 3p$ transitions and compared their work with the experimental results. Chen and Msezane [13] determined the oscillator strength for the $3s \rightarrow 3p$ transition of sodium using the spin-polarized technique of the random phase approximation with exchange (RPAE) and the Hartree-Fock approximation and also identified the minima position. More recently, Miculis and Meyer [14] calculated the absorption cross section of Na ($3p\ ^2P_{3/2}$) into the higher Rydberg state and photoionization cross section

[a] e-mail: baig@qau.edu.pk
[b] Physics Department, UAJK, Muzaffarabad.

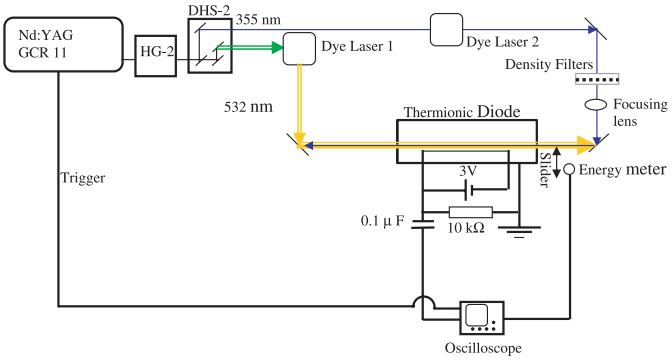

Fig. 1. A schematic diagram of the experimental set-up.

as a function of photoelectron energy and also calculated the Einstein coefficients for spontaneous emission of the $3p_{3/2}$ ns and $3p_{3/2}$ nd Rydberg transitions.

In the present work we have recorded the $3p$ ns, nd series attached to the first ionization threshold using two-step excitation from the $3p$ $^2P_{3/2}$ and $3p$ $^2P_{1/2}$ intermediate states. The photoionization cross section at the first ionization threshold is determined using the saturation technique and subsequently the f-values of the Rydberg transitions have been extracted and are compared with the available literature values.

2 Experimental set-up

The basic experimental arrangement to record the Rydberg series, to measure the photoionization cross section and the oscillator strengths of sodium is similar as described in our earlier work [15–17] is shown in Figure 1. We have used a Nd:YAG laser system (Spectra, GCR-11), operated in the Q-Switched mode, for pumping locally made Hanna type dye lasers [18]. Sodium vapor were produced in a thermionic diode composed of a stainless steel tube 48 cm long, 3 cm in diameter and 1 mm wall thickness. About 20 cm of the central part of the tube was heated by a clamp-shell oven operating at ≈640 K that corresponds to ≈0.2 Torr vapor pressure of sodium. Argon gas at a pressure of ≈0.5 Torr was used as a buffer gas. The temperature was monitored by a Ni-Cr-Ni thermocouple and was maintained with in ±1% by a temperature controller. A 0.2 mm thick tungsten wire, stretched axially along the tube was heated by a separate regulated power supply that served as cathode for the ion detection.

The experiments were performed using a two-step excitation technique. The first dye laser, charged with R590 dye dissolved in methanol and pumped by the SHG (532 nm) of the Nd:YAG laser was used to excite the atoms from the $3s$ $^2S_{1/2}$ ground state to the $3p$ $^2P_{3/2}$ state at 16973.37 cm^{-1} (≈589 nm) in the first experiment and to the $3p$ $^2P_{1/2}$ state at 16956.17 cm^{-1} (≈589.6 nm) in the second experiment. In the second step the second laser, which is a mixture of Stilbene-420 and LD-390 pumped by the third harmonic (355 nm) of the Nd:YAG laser, delayed by a few ns and overlapped with the first laser is used to register the nd and ns Rydberg series of sodium

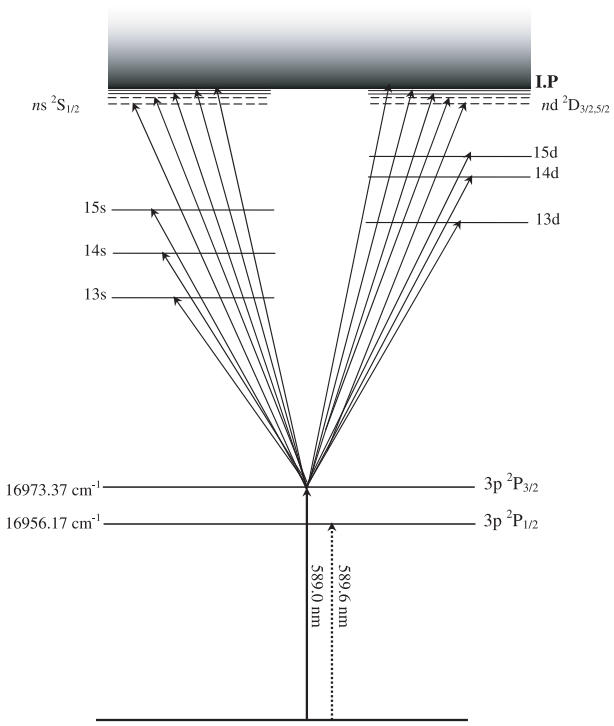

Fig. 2. A schematic energy level diagram of sodium showing the relevant participating levels in the excitation scheme. The level energies are taken from the NIST data [25].

covering wavelength range from 439 nm to the first ionization limit. The natural lifetime of the $3p$ $^2P_{3/2}$ state of Na is 16 ns [19] and the second laser is delayed by approximately 4 ns. Obviously some decay of this state does occur before the arrival of the second laser pulse, but it is negligible [20]. Therefore, the temporal overlapping of both the laser pulses is not very critical. In each of the abovementioned experiments, we have extracted the photoionization cross section at the threshold and used this value of cross section to calibrate the oscillator strengths of the Rydberg transitions. The cross sections were measured using the saturation technique [21]. In each experiment the cross sections are measured by keeping the intensity of the exciting laser fixed while varying the intensity of the ionizing laser using neutral density filters (Edmund Optics). On each insertion, the energy was measured by an energy meter (R-752, Universal Radiometer) and the signal height was recorded on a storage oscilloscope. The ion signal was taken across a 10 kΩ resistor through a 0.1 μF blocking capacitor and was registered on a 200 MHz storage oscilloscope.

3 Results and discussion

In the first set of experiments, we have excited the sodium atoms from the $3s$ $^2S_{1/2}$ ground state to the nd $^2D_{5/2,3/2}$ and ns $^2S_{1/2}$ Rydberg states via the $3p$ $^2P_{3/2}$ intermediate state using the two-step excitation technique. A schematic energy level diagram is shown in Figure 2. The excitation

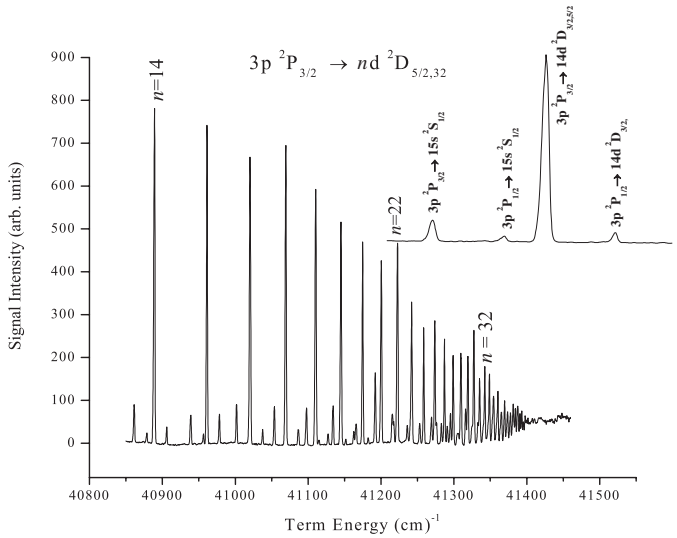

Fig. 3. A portion of the spectrum of sodium showing the $3p$ $^2\mathrm{P}_{3/2} \rightarrow nd$ $^2\mathrm{D}_{5/2,3/2}$ and $3p$ $^2\mathrm{P}_{3/2} \rightarrow ns$ $^2\mathrm{S}_{1/2}$ Rydberg transitions approached from the $3s$ $^2\mathrm{S}_{1/2}$ ground state. An enlarged section of the spectra for the lower member of the series is also inserted indicating the presences of the $3p$ $^2\mathrm{P}_{1/2} \rightarrow 14d$ $^2\mathrm{D}_{3/2}$ and $3p$ $^2\mathrm{P}_{1/2} \rightarrow 15s$ $^2\mathrm{S}_{1/2}$ transitions.

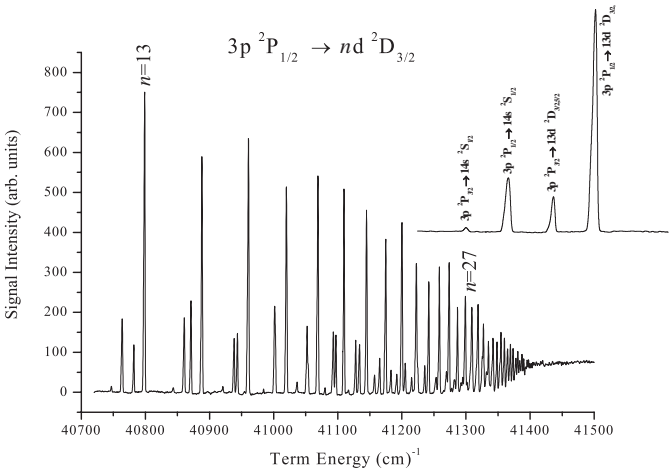

Fig. 4. A portion of the spectrum of sodium showing the $3p$ $^2\mathrm{P}_{1/2} \rightarrow nd$ $^2\mathrm{D}_{3/2}$ and $3p$ $^2\mathrm{P}_{1/2} \rightarrow ns$ $^2\mathrm{S}_{1/2}$ Rydberg transitions approached from the $3s$ $^2\mathrm{S}_{1/2}$ ground state. An enlarged section of the spectra for the lower member of the series is also inserted indicating the presences of the $3p$ $^2\mathrm{P}_{3/2} \rightarrow 13d$ $^2\mathrm{D}_{5/2}$ and $3p$ $^2\mathrm{P}_{3/2} \rightarrow 14s$ $^2\mathrm{S}_{1/2}$ transitions.

spectrum obtained by scanning the second dye laser from 40850.17 cm^{-1} to 41459.74 cm^{-1} is shown in Figure 3. An enlarged portion of the spectra for the lower members of the series is shown as an insert in Figure 3. It is interesting to note that although the first laser which was tuned to achieve the $3p$ $^2\mathrm{P}_{3/2}$ intermediate state only and correspondingly the $3p$ $^2\mathrm{P}_{3/2} \rightarrow nd$ $^2\mathrm{D}_{5/2,3/2}$ and $3p$ $^2\mathrm{P}_{3/2} \rightarrow ns$ $^2\mathrm{S}_{1/2}$ Rydberg series were expected, the spectrum also contains the $3p$ $^2\mathrm{P}_{1/2} \rightarrow nd$ $^2\mathrm{D}_{3/2}$ and $3p$ $^2\mathrm{P}_{1/2} \rightarrow ns$ $^2\mathrm{S}_{1/2}$ states. The appearance of the series from both the multiplets may be attributed to the "collisional processes" that cause decay from the $^2\mathrm{P}_{3/2}$ to the $^2\mathrm{P}_{1/2}$ state. It is due to the fact that at high temperature if the $3p$ $^2\mathrm{P}_{3/2}$ state has been resonantly excited, the collisional redistribution of the population can populate the $3p$ $^2\mathrm{P}_{1/2}$ state as well [22]. It is observed that the nd and ns series excited from the $3p$ $^2\mathrm{P}_{1/2}$ intermediate state possess much lower intensity as compared to that of the $3p$ $^2\mathrm{P}_{3/2}$ state (see Fig. 3). According to the intensity rule in LS-Coupling, the transition probability of the excited states originating from a common level is proportional to their statistical weights [23] and for the transitions $\mathrm{S}_{1/2} \rightarrow \mathrm{P}_{3/2}$ and $\mathrm{S}_{1/2} \rightarrow \mathrm{P}_{1/2}$ the ratio is 2:1. The transition probability of the $3p$ $^2\mathrm{P}_{3/2}$ state is expected to be twice to that from the $3p$ $^2\mathrm{P}_{1/2}$ state. Moreover, the nd series in the spectrum is dominant over the ns series for both of the $3p$ components which are in accordance to the allowed dipole transition rules which implies that a transition in which the orbital and total angular momentum quantum number change in the same direction is more probable than a transition in which both the quantum numbers change in the opposite directions. Therefore the strong Rydberg series accessed from the $3p$ $^2\mathrm{P}_{3/2}$ intermediate state is assigned as nd $^2\mathrm{D}_{5/2,3/2}$ ($13 \leqslant n \leqslant 48$) and the other series which is about four times weaker in intensity than the nd series is assigned as ns $^2\mathrm{S}_{1/2}$ ($14 \leqslant n \leqslant 39$). It is also observed from the recorded Rydberg series, that initially the ns and nd series excited from both the $3p$ multiplets $^2\mathrm{P}_{3/2}$ and $^2\mathrm{P}_{1/2}$ are distinguishable at lower quantum number n, but as the principal quantum number increases the ns series excited from the $3p$ $^2\mathrm{P}_{1/2}$ state tends to mix with the nd series excited from the $3p$ $^2\mathrm{P}_{3/2}$ state. Similarly the nd series signal due to excitation from $3p$ $^2\mathrm{P}_{1/2}$ mixes with the ns series due to the $3p$ $^2\mathrm{P}_{3/2}$ state. This mixing/overlap occur due to the bandwidth of second laser which is $\approx$0.3 cm^{-1} and as long as it is less than the energy separation between the ns and nd series components, they remain distinguishable.

In the second set of experiments, the atoms are excited from the $3s$ $^2\mathrm{S}_{1/2}$ ground state to the nd $^2\mathrm{D}_{3/2}$ and ns $^2\mathrm{S}_{1/2}$ Rydberg states via the $3p$ $^2\mathrm{P}_{1/2}$ intermediate state. The first dye laser is tuned to the $3p$ $^2\mathrm{P}_{1/2}$ at 16956.17 cm^{-1} (589.6 nm) and the second dye laser (ionizing), delayed by a few ns, is overlapped with the first dye laser and scanned in the energy range from 40 715 cm^{-1} to 41 500 cm^{-1}. The spectra recorded at stabilized temperature and pressure is shown in Figure 4. An enlarged portion of the spectra for the lower members of the series is also shown as an insert in this figure. It is obvious from the figure that at low pressure of the buffer gas the dipole allowed transitions $3p$ $^2\mathrm{P}_{1/2} \rightarrow nd$ $^2\mathrm{D}_{3/2}$ are sharp and correspondingly have higher peak intensity as compared to the ionization signals that originate due to $3p$ $^2\mathrm{P}_{3/2} \rightarrow nd$ $^2\mathrm{D}_{5/2,3/2}$ transition. As the first laser is tuned to the $^2\mathrm{P}_{1/2}$ intermediate state, one can observe only the $3p$ $^2\mathrm{P}_{1/2} \rightarrow nd$ $^2\mathrm{D}_{3/2}$ transition and the $3p$ $^2\mathrm{P}_{3/2} \rightarrow nd$ $^2\mathrm{D}_{5/2}$ transition should not have been

there. However it is evident from Figure 4 that both the lines are present. There are a number of possible mechanisms for the occurrence of the transitions from both the $3p\ ^2P_{3/2}$ and $^2P_{1/2}$ components.

(a) The bandwidth of the first laser may be sufficiently large so that its wings can overlap and populate $^2P_{3/2}$. In the present work, the laser line width ($\leqslant 0.3$ cm^{-1}) is much smaller than the splitting between the $^2P_{1/2}$ and $^2P_{3/2}$ states (17.198 cm^{-1}). Therefore this possibility can be discarded.
(b) The intensity of the first laser is sufficiently large that laser energy density causes AC Stark splitting or shifts. This basis can also be ruled out as the intensity of the first step exciting laser is kept very low.
(c) The collisional redistribution of population may populate the $3p\ ^2P_{3/2}$ level if $3p\ ^2P_{1/2}$ is excited resonantly, provided the pressure and/or the temperature in the interaction zone are high. In the present work, the temperature in the cell is kept at 640 K that corresponds to 0.2 Torr vapor pressure of sodium.

Burkhardt et al. [22] and Zhang et al. [24] reported the appearance of such transitions in sodium Rydberg series. It seems that the optical collisions are responsible for the occurrence of these transitions.

The absolute term energies of all the excited states are calculated by adding the laser excitation energy to the energy of the relevant intermediate state. The quantum defects associated with different energy states are calculated using the standard Rydberg formula

$$E_n = IP - \frac{R_y}{(n-\mu_\ell)^2} \tag{1}$$

where R_y is the mass corrected Rydberg constant of sodium 109734.698 cm^{-1}, E_n (cm^{-1}) is the energy corresponding to the Rydberg levels, μ_ℓ is the quantum defect and IP is the ionization potential to 41449.45 cm^{-1} [25] for sodium. The $nd\ ^2D_{5/2,3/2}$ and $ns\ ^2S_{1/2}$ series are observed up to $n = 48$ and $n = 39$ respectively. The Rydberg series can be extended to a much higher principal quantum number by improving the laser bandwidth and signal to noise ratio. However, the main objectives of the present work were to measure the oscillator strengths of the above-mentioned Rydberg transitions rather than to extend the series to higher n-values.

In the second part of our work, we have measured the absolute photoionization cross section at the first ionization threshold using the saturation technique as described by Burkhardt et al. [21] who applied the two-step ionization technique to measure the absolute cross section from the excited states of sodium, potassium and barium. An empirical relation was developed to determine the cross section at the ionizing laser wavelength as;

$$Z = \frac{Q}{eV_{vol}} = N_{ex}\left[1 - \exp\left(-\frac{\sigma U}{2\hbar\omega A}\right)\right] \tag{2}$$

where Z is the total number of ions collected per unit volume, e (coulomb) is the electronic charge, N_{ex} (cm^{-3}) is the density of excited atoms, A (cm^2) is the cross sectional area of the ionizing laser beam, U (Joule) is the total energy per ionizing laser pulse, $\hbar\omega$ (Joule) is the energy per photon of the ionizing laser beam, V_{vol} (cm^3) is the laser interaction volume and σ (cm^2) is the absolute cross section for photoionization.

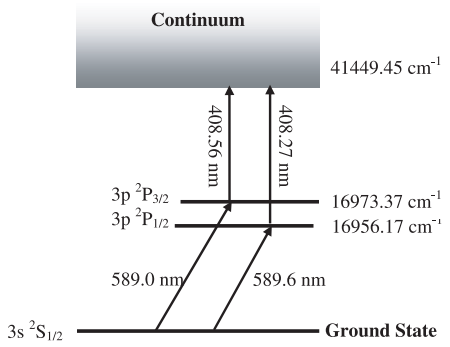

Fig. 5. Energy level diagram showing the two-step excitation and ionization paths employed to measure the photoionization cross section at the first ionization threshold.

Subsequently, He et al. [26] reported the absolute photoionization cross section of the $6s6p\ ^1P_1$ excited state of barium. Their method for determining the photoionization cross section is an extension of the saturation technique described by Burkhardt et al. [21] and accounting the effects for the Gaussian laser intensity distribution. Mende et al. [27] modified equation (2) and determined the photoionization cross section using the equation:

$$Z = N\int_V \left(1 - \exp\left(-\frac{1}{2}\sigma\Phi_{Ph}\right)\right)dV. \tag{3}$$

Here Z is the total charge per pulse, σ is the cross section for the photoionization, Φ_{Ph} is the time-integrated number of photons spatially distributed over the area of the ionizing laser pulse:

$$\Phi_{Ph} = \frac{E}{h\upsilon}\frac{1}{\pi\Delta\rho^2}\exp\left\{-\left(\frac{\rho}{\Delta\rho}\right)^2\right\} \tag{4}$$

here E is the total energy per laser pulse, $h\nu$ is the photon energy and $\Delta\rho$ is the half width of the distribution profile. An expression similar to that of Burkhardt et al. [21] was used by Xu et al. [28] to measure the photoionization cross sections of the autoionizing states of lutetium and by Saleem et al. [29] to measure the photoionization of the $2p$ states of lithium.

In the present experiment, we have determined the photoionization cross section using equation (2) under the best alignment conditions for the Gaussian laser intensity distribution. In the first set of experiments, we have measured the photoionization cross section from the $3p$ excited state of sodium up to the first ionization threshold. A schematic diagram of the pertinent transitions is shown in Figure 5. From the $3s\ ^2S_{1/2}$ ground state, the sodium atoms can be promoted either to the $3p\ ^2P_{1/2}$ or to the $3p\ ^2P_{3/2}$ state using the dye laser at 589.6 nm or

589.0 nm respectively. As the first dye laser is pumped by the second harmonic (532 nm) of the Nd:YAG laser thus the laser light is linearly polarized in the z-direction. Consequently, the accessible transitions follow $\Delta m_j = 0$ selection rules. The upper states possess $m_j = +1/2$ and $-1/2$. In the second step the atoms from either the $^2P_{1/2}$ or $^2P_{3/2}$ state are ionized by the second dye laser pumped by the third harmonic (355 nm) of the same Nd:YAG laser set either at 408.27 nm or 408.56 nm. The ionizing laser is also linearly polarized but its direction of polarization is horizontal with respect to the first step dye laser. Keeping the intensity of the exciting laser fixed and varying the intensity of the ionizing laser, using the neutral density filters, we have registered the corresponding ion signals. The excitation laser beam has a spot diameter ∼1.3 mm and the area of the overlap region in the confocal limit is calculated using the relation [3,30,31]:

$$A = \pi r_0^2 \left[1 + \left[\frac{\lambda \ell}{\pi r_0^2}\right]^2\right] \quad (5)$$

here $r_0 = f\lambda/(\pi r_s)$ is the beam waist, r_s is the spot size of the beam on the focusing lens and ℓ is taken as the effective length of the heating zone. The cross sectional area of the ionizing lasers at 408.27 nm and 408.56 nm is calculated as 0.0026(1) cm^2 using the spot size of 0.02 cm at a focal length of 50 cm. The intensity of the first dye laser beam was kept fixed while the intensity of the ionizing laser beam was varied by inserting neutral density filters (Edmond Optics) on its optical path. The ionizing dye laser energy was measured by an energy meter (R-752, Universal Radiometer) within ±5% variation. We have registered the signal intensities against the pulse energies of the ionizing laser on a storage oscilloscope and stored on a computer for further processing. Typical data for the photoionization of the $3p\ ^2P_{3/2}$ and $3p\ ^2P_{1/2}$ levels are shown in Figures 6a and 6b. The dots including 5% error bars represent the experimental data points. The solid line, which passes through the data points, is a least square fit of equation (2). It is evident from Figures 6a and 6b that as the laser intensity increases; the ion signal increases up to certain value and then the signal stops increasing any further. At this point the photoionization from the first excited state reaches its maximum and saturation sets in. At saturation, the photon flux of the ionizing laser equalizes the population of the intermediate levels. The fitting of the experimental data for the $3p\ ^2P_{1/2}$ and $3p\ ^2P_{3/2}$ level yields the value of the photoionization cross section at the first ionization threshold as 6.7(1.1) Mb and 7.9(1.3) Mb respectively. The estimated uncertainty in the value of the photoionization cross sections σ is ±17%, which is due to the experimental errors in the measurements of the laser energy, diameter of the laser beam and calibration of the detection system.

The photoionization cross sections of sodium at the first ionization threshold have been measured by a number of groups ([17] and reference therein). Rothe [32] reported the cross section of the $3p$ levels as 7.63(90) Mb whereas, Aymar et al. [33] calculated its value as 7.38 Mb.

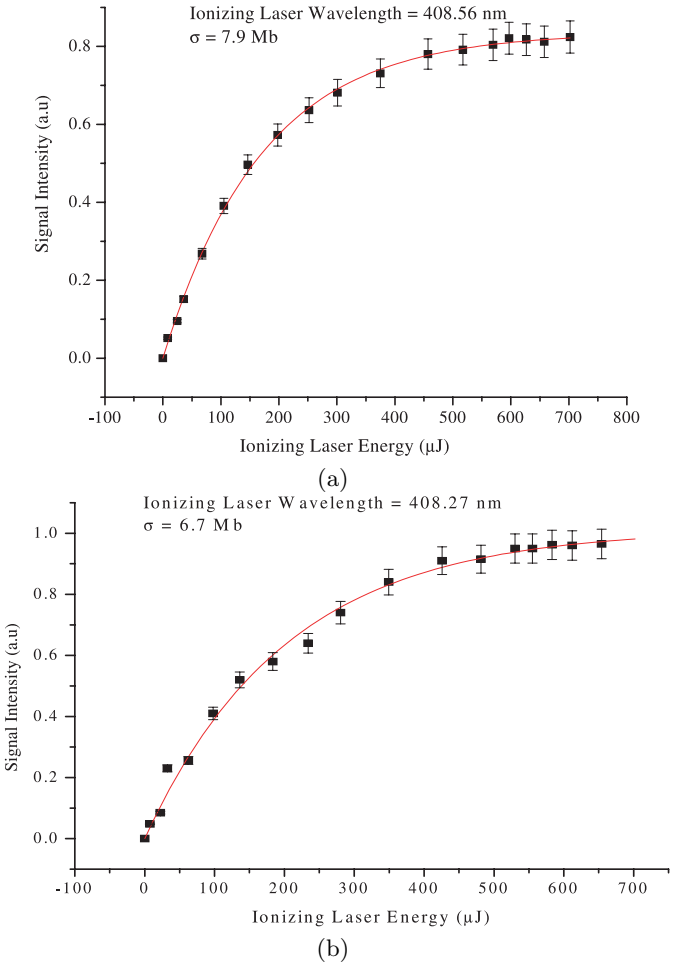

Fig. 6. The photoionization signals plotted against the ionization laser energy (a) from the $3p\ ^2P_{3/2}$ (b) from the $3p\ ^2P_{1/2}$ states. The solid line is the least square fit of equation (2) to the observed data for extracting the values of cross section σ (Mb) at the first ionization threshold.

Preses et al. [34] used the two-step excitation scheme to determine the photoionization cross section from the $3p\ ^2P_{3/2}$ state of Na up to the first ionization threshold, with the help of two antiparallel, interpenetrating pulsed laser beams pumped by the frequency doubled (532 nm) and tripled (355 nm) outputs of a Nd:YAG laser. They determined the value of the cross section as 8.5 Mb with an estimated uncertainty of about 25%. Petrov et al. [35] theoretically calculated the photoionization cross section of the $3p\ ^2P_{3/2}$ state about ≈8 Mb. Wippel et al. [36], using the trapping-technique, trapped a fraction of Na atoms in the $3p\ ^2P_{3/2}$ excited state and then ionized them with a laser adjusted at ∼407.8 nm. They determined the value of the cross section at threshold as 6.9(1) Mb. Miculis and Meyer [14] calculated the photoionization cross section from $3p\ ^2P_{3/2}$ at and above threshold and our experimental value is in excellent agreement to their calculated value.

Measurements of the optical oscillator strength of electronic transitions have great significance in areas such as

Table 1. Optical oscillator strengths corresponding to the $nd\ ^2D_{5/2,3/2}$ transitions excited from the $3p\ ^2P_{3/2}$ and $3p\ ^2P_{1/2}$ intermediate states of sodium.

Quantum number	$3p\ ^2P_{3/2} \rightarrow nd\ ^2D_{5/2,3/2}$		$3p\ ^2P_{1/2} \rightarrow nd\ ^2D_{3/2}$	
	Wavelength (nm)	Oscillator strengths	Wavelength (nm)	Oscillator strengths
13	419.59	2.63×10^{-4}	419.30	2.48×10^{-4}
14	418.02	2.44×10^{-4}	417.73	2.23×10^{-4}
15	416.76	2.26×10^{-4}	416.47	2.12×10^{-4}
16	415.74	2.05×10^{-4}	415.45	1.70×10^{-4}
17	414.89	1.67×10^{-4}	414.60	1.58×10^{-4}
18	414.19	1.39×10^{-4}	413.90	1.17×10^{-4}
19	413.59	1.18×10^{-4}	413.30	1.17×10^{-4}
20	413.08	9.33×10^{-5}	412.79	8.53×10^{-5}
21	412.65	8.12×10^{-5}	412.36	9.45×10^{-5}
22	412.27	8.37×10^{-5}	411.98	7.83×10^{-5}
23	411.94	7.97×10^{-5}	411.65	6.00×10^{-5}
24	411.66	5.64×10^{-5}	411.37	6.75×10^{-5}
25	411.40	6.29×10^{-5}	411.11	6.54×10^{-5}
26	411.18	5.25×10^{-5}	410.88	4.47×10^{-5}
27	410.97	4.23×10^{-5}	410.68	5.34×10^{-5}
28	410.79	4.54×10^{-5}	410.51	4.68×10^{-5}
29	410.63	4.65×10^{-5}	410.35	5.04×10^{-5}
30	410.49	3.47×10^{-5}	410.21	3.50×10^{-5}
31	410.36	3.89×10^{-5}	410.07	2.25×10^{-5}
32	410.24	3.02×10^{-5}	409.95	3.30×10^{-5}
33	410.13	2.96×10^{-5}	409.84	2.32×10^{-5}
34	410.04	2.87×10^{-5}	409.74	3.21×10^{-5}
35	409.94	2.58×10^{-5}	409.66	2.53×10^{-5}
36	409.86	2.10×10^{-5}	409.57	1.55×10^{-5}
37	409.78	2.21×10^{-5}	409.50	2.21×10^{-5}
38	409.72	1.56×10^{-5}	409.43	2.18×10^{-5}
39	409.65	1.57×10^{-5}	409.36	2.31×10^{-5}
40	409.59	1.15×10^{-5}	409.31	1.22×10^{-5}
41	409.53	1.29×10^{-5}	409.25	1.11×10^{-5}
42	409.48	1.78×10^{-5}	409.20	1.52×10^{-5}
43	409.43	9.02×10^{-6}	409.15	9.36×10^{-6}
44	409.39	7.02×10^{-6}	409.11	1.02×10^{-5}
45	409.35	1.24×10^{-5}	409.06	6.54×10^{-6}
46	409.31	5.95×10^{-6}	409.02	7.65×10^{-6}
47	409.28	7.57×10^{-6}	408.99	6.37×10^{-6}
48	409.25	4.24×10^{-6}	408.95	7.48×10^{-6}
49			408.92	8.87×10^{-6}
50			408.90	6.20×10^{-6}

radiation physics, plasma physics and astrophysics. The oscillator strengths of discrete states provide a sensitive test for atomic structure calculation. This information is very useful for developing the theoretical models involving electronic transitions induced by the energetic radiation. Mende and Kock [37] developed an experimental technique to determine the absolute oscillator strength of the Rydberg transitions for medium to high principal quantum numbers. Absolute value of the photoionization cross section measured at the ionization threshold was used to calibrate the f-values of the Rydberg transitions. A simple relation was obtained [37] between the f-values of the Rydberg transitions and the photoionization cross section measured at a particular frequency as:

$$f_{\ell n} = 3.77 \times 10^5 \frac{S^{\ell n}}{S^{1+}} \frac{\nu^{\ell n}}{\nu^{1+}} \sigma \qquad (6)$$

where $f_{\ell n}$ is the oscillator strength of a Rydberg transition, which is directly proportional to the photoionization cross section σ measured at the ionization threshold frequency υ^{1+}. The quantity S^{1+} is the ion signal at the ionization threshold and $S^{\ell n}$ is the integrated ion signal intensity for the nth Rydberg transition. The total line absorption $S^{\ell n}$ is obtained by integration as described by Mende and Kock [37]. It is equal to the peak-values time half width i.e. $S^{\ell n} = \textit{Signal Intensity} \times c\,\Delta k$, where "$c$" is speed of light and k is in wave number (cm^{-1}). We have determined the oscillator strengths of the nd Rydberg transitions of sodium by employing equation (6). The f-values of the $3s^2S_{1/2} \rightarrow 3p\ ^2P_{3/2} \rightarrow nd\ ^2D_{5/2,3/2}$ Rydberg transitions (two-step excitation) are calibrated with the photoionization cross section 7.9 (1.3) Mb measured at the first ionization threshold from the $3p\ ^2P_{3/2}$ state

(see above). Similarly we have determined the f-values of the $3s^2S_{1/2} \rightarrow 3p\ ^2P_{1/2} \rightarrow nd\ ^2D_{3/2}$ Rydberg transitions by calibration with the photoionization cross section 6.7(1.1) Mb measured at the first ionization threshold from the $3p\ ^2P_{1/2}$ state. The numerical data are presented in Table 1. In the first and second columns the wavelengths and the oscillator strengths corresponding to $3p\ ^2P_{3/2} \rightarrow nd\ ^2D_{5/2,3/2}$ transitions are given while in the third and fourth columns, the wavelengths and the oscillator strengths corresponding to $3p\ ^2P_{1/2} \rightarrow nd\ ^2D_{3/2}$transitions are listed respectively.

In Figures 7a and 7b, the f-values of the Rydberg transitions are plotted against their effective quantum numbers in a double logarithmic scale. The experimental data points are fitted to an expression: $f_n = K/(n^*)^\alpha$ which yields the values of α as 2.88 for the $3p\ ^2P_{3/2} \rightarrow nd\ ^2D_{5/2,3/2}$ series and 2.44 for the $3p\ ^2P_{1/2} \rightarrow nd\ ^2D_{3/2}$ series. The f-values for an unperturbed Rydberg series, that follows the n^{-3} scaling law [20], are also plotted. The energy positions of the $nd\ ^2D_{5/2,3/2}$ Rydberg states are well documented but the data on the f-values of the transition lines are available only for the lower members of the series [19]. Gallagher et al. [38] measured the radiative lifetimes of the ns ($7 \leqslant n \leqslant 13$) and nd ($5 \leqslant n \leqslant 13$) Rydberg series using two-step excitation via $3p\ ^2P_{3/2}$ intermediate state. Subsequently, Spencer et al. [39] measured the lifetimes of sodium s and d levels in the range $17 < n < 28$ in cooled environment and taking into account the life time shortening due to the blackbody radiation as reported earlier by Gallagher and Cooke [40] and Cooke and Gallagher [41]. For the lower n-values ($5 \leqslant n \leqslant 13$), the life-time data for the $3p\ ^2P_{3/2} - nd$ transitions by Gallagher et al. [38] and for the higher n-values for ($17 < n < 28$) the data of Spencer et al. [39] follow $(n^*)^3$ scaling law. The life times of the sodium nd states were represented by a relation [2]: $\tau = \tau_0(n^*)^\alpha$ with the values of $\tau_0 = 0.96$ (ns) and $\alpha = 2.99$.

A plot of our results on the f-values along with that of the data of recent theoretical results of Miculis and Meyer [14] is shown in Figure 8. In this paper the transition probabilities of $3p\ ^2P_{3/2} \rightarrow nd\ ^2D_{3/2}$ Rydberg transitions of sodium were reported and it was inferred that the values for the $3p\ ^2P_{3/2} \rightarrow nd\ ^2D_{5/2}$ transitions can be calculated by multiplying it with six. We have calculated the f-values from the listed Einstein coefficients by Miculis and Meyer [14] using the following relation [19]:

$$f = 1.599 \times 10^{-16}\lambda^2(g_k/g_i)A_{ki}. \qquad (7)$$

Since in our experiment the $nd\ ^2D_{3/2}$ and $nd\ ^2D_{5/2}$ components have not been resolved therefore we have taken an average value of both the components from [14] and compared with our experimental data. Our data at the lower n-values slightly deviate from that of Miculis and Meyer [14]. It is to be remarked that the technique for the measurement of oscillator strengths of the Rydberg transitions applied in the present work and described by Mende et al. [37] is applicable from medium to high principal quantum numbers. This is because of the collisional ionization probability which approaches unity for the highly

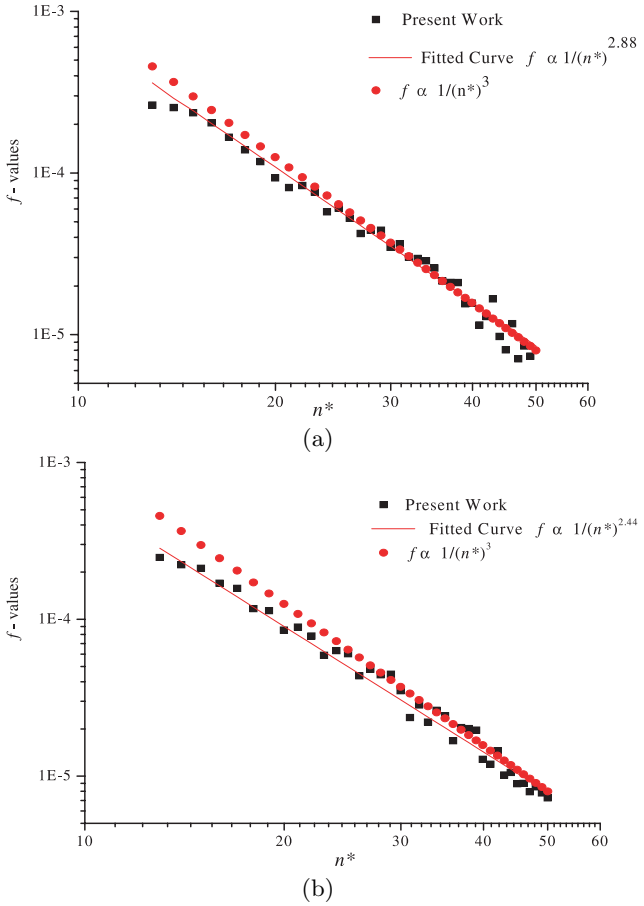

Fig. 7. (a, b) A plot of the oscillator strengths of the $nd\ ^2D_{5/2,3/2}$ Rydberg transitions versus the effective quantum number n^*. The solid line that passes through the experimental data points, indicating that the f-values of $3p\ ^2P_{3/2} \rightarrow nd\ ^2D_{5/2,3/2}$ Rydberg transitions decreases as $(n^*)^{-2.88}$ while in case of $3p\ ^2P_{1/2} \rightarrow nd\ ^2D_{3/2}$ transitions; it decreases as $(n^*)^{-2.44}$.

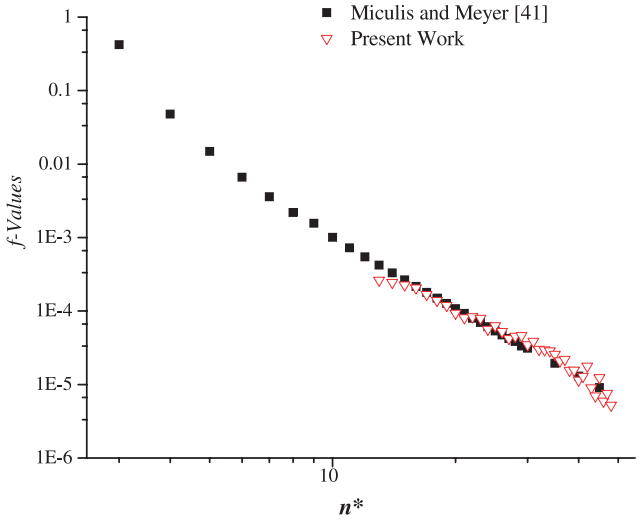

Fig. 8. A plot of the f-values corresponding to the $3p\ ^2P_{3/2} \rightarrow nd\ ^2D_{5/2,3/2}$ transitions versus the effective quantum number (n^*) along with the previous work of Miculis and Meyer [14].

excited Rydberg states. The deviation in the measured values around $n = 13$ is attributed to the limitation of the technique. A similar behavior of deviations at the lower members of the Rydberg series has been observed in the spectra of lithium, potassium and strontium.

In conclusion, we have measured the photoionization cross section from the $3p\ ^2P_{3/2}$ and $3p\ ^2P_{1/2}$ intermediate states at the first ionization threshold as 7.9(1.3) Mb and 6.7(1.1) Mb respectively. The cross section from the $3p\ ^2P_{1/2}$ at the first ionization threshold is reported for the first time. The f-values of the Rydberg transitions have been determined up to higher n-values, for the first time, that are compared with the earlier data. The uncertainty in the measured f-values does not exceed 20%. There is a further room for improvements in this method, particularly in the measurement of spatial distribution of laser photon flux and a precise value of the interaction region.

The present work was financially supported by the Higher Education Commission (HEC), Pakistan Science Foundation and the Quaid-i-Azam University, Islamabad, Pakistan. M.A. Kalyar, M. Rafiq. N. Amin and Sami-ul-Haq are grateful to the HEC for the grant of Ph.D. scholarship under the Indegenous scheme.

References

1. V.S. Letokhov, *Laser Photoionization Spectroscopy* (Academic Press, Florida, 1987)
2. T.F. Gallagher, *Rydberg Atoms* (Cambridge University Press, Cambridge, 1994)
3. W. Demtroder, Laser *Spectroscopy* (Berlin, Springer, Berlin, 1996)
4. J.P. Connerade, *Highly Excited Atoms* (Cambridge University Press, UK, 1998)
5. J. Berkowitz, *Atomic and Molecular Photoabsorption* (Academic Press, New York, 2002)
6. S.T. Manson, Phys. Rev. A **3**, 1260 (1971)
7. J.C. Weisheit, Phys. Rev. A **5**, 4 (1972)
8. T. Shuttleworth, W.R. Newell, A.C.H. Smith, J. Phys. B: At. Mol. Opt. Phys. **10**, 3307 (1977)
9. L. Vuskovic, S.K. Srivastava, J. Phys. B: At. Mol. Opt. Phys. **13** , 4849 (1980)
10. C. Barrientos, I. Martin, Can. J. Phys. **65**, 435 (1987)
11. J. Mitroy, Phys. Rev. A **35**, 10 (1987)
12. C.E. Bielschowsky, C.A. Lucas, G.G.B. de Souza, Phys. Rev. A **43**, 5975 (1991)
13. Z. Chen, A. Msezane, Phys. Rev. A **61**, 030703 (2000)
14. K. Miculis, W. Meyer, J. Phys. B: At. Mol. Opt. Phys. **38**, 2097 (2005)
15. M. Anwar-ul-Haq, Shaukat Mahmood, M. Riaz, R. Ali, M.A. Baig, J. Phys. B: At. Mol. Opt. Phys. **38**, S77 (2005)
16. M. Riaz, Shaukat Mahmood, M. Anwar-ul-Haq, M.A. Baig, Opt. Commun. **244**, 339 (2005)
17. N. Amin, S. Mahmood, M. Anwar-ul-Haq, M. Riaz, M.A. Baig, Eur. Phys. J. D **37**, 23 (2006)
18. D. Hanna, P.A. Karkainen, R. Wyatt, Opt. Quantum Electron **7**, 115 (1975)
19. W.L. Wiese, M.W. Smith, B.M. Miles, *Atomic Transition Probabilities* (1969), Vol. II
20. T.F. Gallagher, S.A. Edelstein, R.M. Hill, Phys. Rev. A **11**, 1504 (1975)
21. C.E. Burkhardt, J.L. Libbert, J. Xu, J.J. Leventhal, J.D. Kelley, Phys. Rev. A **38**, 11 (1988)
22. C.E. Burkhardt, M. Ciocca, W.P. Garver, J.J. Leventhal, J.D. Kelley, Phys. Rev. Lett. **57**, 1562 (1986)
23. H.E. Bethe, E.E. Salpeter, *Quantum Mechanics of One and Two Electron Atoms* (Springer-Verlag, Berlin, 1957)
24. J. Zhang, P. Lambropoulos, D. Zei, R.N. Compton, J.A.D. Stockdale, Z. Phys. D: At. Mol. Clust. **23**, 219 (1992)
25. NIST data base `www.physics.nist.gov` (2005)
26. L.W. He, C.E. Burkhardt, M. Ciocca, J.J. Leventhal, Phys. Rev. Lett. **67**, 2131(1991)
27. W. Mende, K. Bartschat, M. Kock, J. Phys. B: At. Mol. Opt. Phys. **28**, 2385 (1995)
28. C.B. Xu, X.Y. Xu, H. Ma, L.Q. Li, W. Huang, D.Y. Chen, F.R. Zhu, J. Phys. B: At. Mol. Opt. Phys. **26**, 2827 (1993)
29. M. Saleem, N. Amin, S. Hussain, M. Rafiq, Shaukat Mahmood, M.A. Baig, Eur. Phys. J. D **38**, 277 (2006)
30. J.M. Song, T. Inoue, H. Kawazumi, T. Ogawa, Analytical Sciences **15**, 601 (1999)
31. R. Guenther, *Modern Optics* (John Wiley & Sons, 1990)
32. D.E. Rothe, J. Quant. Spectrosc. Radiat. Transfer **9**, 49 (1969)
33. M. Aymar, E. Luc-Koenig, F.C. Farnoux, J. Phys. B: At. Mol. Phys. **9**, 8 (1976)
34. J.M. Preses, C.E. Burkhardt, R.L. Corey, D.L. Earsom, T.L. Daulton, W.P. Garver, J.J. Leventhal, A.Z. Msezane, S.T. Manson, Phys. Rev. A **32**, 1264 (1985)
35. I.D. Petrov, V.L. Sukhorukov, E. Leber, H. Hotop, Eur. Phys. J. D **10**, 53 (2000)
36. V. Wippel, C. Binder, W. Huber, L. Windholz, M. Allegrini, F. Fuso, E. Arimondo, Eur. Phys. J. D **17**, 285 (2001)
37. W. Mende, M. Kock, J. Phys. B: At. Mol. Opt. Phys. **29**, 655 (1996)
38. T.F. Gallagher, S.A. Edelstein, R.M. Hill, Phys. Rev. A **11**, 1504 (1975)
39. W.P. Spencer, A.G. Vaidyanathan, D. Kleppner, T.W. Ducas, Phys. Rev. A **24**, 2513 (1981)
40. T.F. Gallagher, W.E. Cooke, Phys. Rev. Lett. **13**, 835 (1979)
41. W.E. Cooke, T.F. Gallagher, Phys. Rev. A **21**, 588 (1980)